15 May 1994

OPTICS COMMUNICATIONS

ELSEVIER

Optics Communications 108 (1994) 176–184

Full length article

Multi-colour-pumped oscillator in photorefractive $BaTiO_3$

M. Kaczmarek [1], L. Solymar, P. Pun

Department of Engineering Science, University of Oxford, Parks Road, Oxford, OX1 3PJ, UK

Received 12 March 1993; revised manuscript received 27 May 1993

Abstract

A photorefractive multi-colour-pumped oscillator is described. Oscillation beams, generated by three input beams of different wavelengths, show the effect of competition resulting in their different build-up and behaviour. A theoretical model, based on two sets of coupled differential equations gives good agreement with experimental data.

1. Introduction

The idea of coupling between incoherent optical beams has been extensively explored in the past few years. Photorefractive materials are ideally suited for such applications owing to their large nonlinearities and sensitivity within the whole visible and near-infrared spectrum. A number of photorefractive phase conjugators and oscillators have been suggested and developed [1–10], based mainly on the four-wave mixing process. They have great potential for applications in optical information processing, controllable light modulation and filtering, as well as for laser locking [9–12].

Two of the most popular configurations are: the double-phase-conjugate mirror (DPCM) and the double-colour-pumped oscillator (DCPO). In both of them, two new waves are simultaneously self-generated due to the interaction of two mutually incoherent input beams of the same wavelength (DPCM) [5,9,10] or two input beams of different wavelengths (DCPO) [1,7].

The DPCM process has been extensively studied during the past few years. The most important results include work on such processes as time evolution of the phase conjugate waves [13,14], and the influence of seeding [15]. Moreover, the shape of the phase conjugate beams – a conical or a partial conical ring – and its intensity distribution were investigated both experimentally and theoretically [16,14].

So far, less work has been devoted to the more detailed analysis of the double-colour-pumped oscillation process. However, the experimental [1,7,17–19] and theoretical [7,18] investigations provided a good description of the threshold conditions and power variations of the output oscillation beams.

Our work was aimed at investigating the full potential of the DCPO as an oscillator cross coupling different wavelengths. We modified its standard arrangement by sending an additional, third input beam into a crystal leading to a multi-colour-pumped oscillator (MCPO). As a result, we observed two double-colour-pumped oscillation effects, existing simultaneously within the same crystal and producing, in total, four new oscillation beams. One of our objectives was

[1] On leave from the Department of Physics, A. Mickiewicz University, Poznań, Poland.
Present address: Optoelectronics Research Centre, University of Southampton, Southampton, SO9 5NH, UK.

0030-4018/94/$07.00 © 1994 Elsevier Science B.V. All rights reserved
SSDI 0030-4018(94)00140-P

to verify and elucidate the possibility of mutual influence or competition between the two DCPO processes.

Previous work on multi-wavelength interactions in photorefractive crystals provided us with some important and useful background. It was demonstrated [21] that in the achromatic DPCM, using multi-wavelength input beams, one common grating for all wavelengths can be formed. However, it requires particular care in choosing both a material with suitable dispersion characteristics, and incidence angles. Moreover, the existence of multi-gratings for different pairs of the input wavelengths (via the DPCM or DCPO effect), which are not phase matched can cause a degradation in the diffraction efficiency [21,22]. Multi-wavelength beam fanning [20] was also described, where a destructive competition between gratings set-up by different wavelengths was overcome by the spatial separation of the incident wavelengths or special feedback resonators. Cooperative beam fanning was also observed, i.e. fanning gratings coming from different wavelengths could actually support each other, again utilising the geometry of incidence and material dispersion.

The arrangement we propose includes cross coupling between three single-frequency input beams. The interaction can be successfully modelled on the basis of standard four-wave mixing theory.We have investigated two different set-ups. In the first one, we choose the third input beam to be of a third, different wavelength. In the second one, the third beam had the same wavelength and was *coherent* with one of the input beams. We measured the power of all interacting beams under various experimental conditions. Further, we used numerical modelling to calculate their power to aid the interpretation of the experimental results.

In the next two sections we will concentrate on the experimental and then on the theoretical analysis of the MCPO, discussing and comparing the behaviour of the oscillation beams under different input beams' regimes. In the third section, we will proceed to presenting results obtained from the second arrangement. The important similarities and differences between both set-ups, observed experimentally and predicted by theory, will be described. For both arrangements we will point out the competition effects existing between two double-colour-pumped oscillation effects, and finally indicating novel processing capabilities.

2. Experimental study of the MCPO

The experimental arrangement for the multi-colour-pumped oscillator is drawn schematically in Fig. 1. A HeNe laser operating at 632.8 nm and two argon-ion lasers operating at 514.5 nm and 488 nm provided three input beams (labelled as 2, 4 and 5). A $BaTiO_3$ crystal was used as the photorefractive material. The input beams were arranged in such a way that two of them, blue and red, were incident on the same, 5 × 6 mm face of the $BaTiO_3$ crystal, while the third one, the green one, was directed on the opposite face. The crossing angle between the input blue and the input green was set to 175°. The angle between the input blue and red beam was about 5° in order to create long overlap regions with the green beam. All three pump beams had horizontal (extraordinary) polarisation. The incident and the output beams, reflected from two beam splitters, passed through lenses focusing them on detecting photodiodes. Signals from all seven photodiodes were then sent to a laboratory computer. Each data point recorded was the average of about 100 measurements taken over about a 10 s period.

The interactions between the input blue beam and the green beam, and between the red input beam and the green created two gratings, which were separated in space and had different grating vectors. As a result we observed two DCPO effects, giving rise, in total, to four new oscillation beams: the input blue (beam 4) and the input green (beam 2) provided the oscillation beams in green (beam 3), and in blue (beam 1); the input red (beam 5) and the input green (beam 2) produced the second oscillation beam in green (beam 6), and one in red (beam 7). The propagation paths of the oscillation beams were determined by the crossing angle of the two respective input beams and their difference in wavelength [7]. All four oscillation beams emerged from different points of the crystal and therefore could be measured separately.

In the experiments performed we investigated the variation of the oscillation beam power as a function of input power. In the first experiment, the crystal was pumped with increasing input red power, while the input blue and green were kept constant. In the second

FULL LENGTH ARTICLE

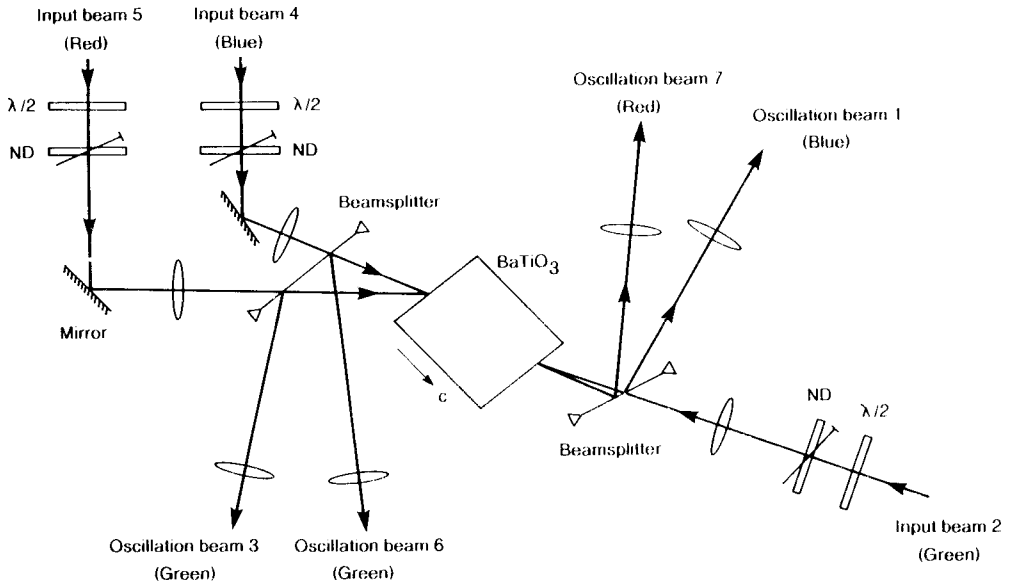

Fig. 1. Experimental arrangement of multi-colour-pumped oscillator. $\lambda/2$: half-wave plate; ND: variable neutral density filter.

one, the input blue power was varying, and the input red and green were constant.

We aimed to observe and examine the mutual influence of the two DCPO effects. To determine this effect quantitatively we carried out the experiment in the following way. The power of each oscillation beam was measured in two different configurations: when only the two input beams generating it were present, and when all three input beams were present. In physical terms, in the first situation only one DCPO effect takes place, whereas in the second two DCPO effects occur. Experimentally, we achieved these two arrangements by simply blocking and unblocking one of the input beams, either blue or red, and measuring simultaneously the power of all beams.

The results we obtained in our experiment indicated that the presence of the additional, third input beam may have an impact on the oscillation beams behaviour. The oscillation beams generated due to the red–green DCPO interaction, i.e. I_7 and I_6 decreased in power in the presence of the third, blue beam. However, the oscillation beams coming from the blue–green DCPO coupling, i.e. I_1 and I_3 were not affected by the additional input red beam. These "competition" effects will now be analysed theoretically, with the aim being to provide a better understanding of the interactions occurring. We will model this multi-colour phenomenon numerically and the next section is devoted to the explanation of the model we used.

3. Numerical modelling

Fig. 2 presents the geometry of the wave mixing responsible for the multi-colour pumped oscillations. The two DCPO phenomena were produced in two regions inside the crystal. The grating induced in each region is responsible for diffracting only the two respective input beams into the two oscillation beams, and there is no direct coupling between waves generated due to each of the interactions. As we discussed in the preceding section, input beams I_2 (green) and I_4 (blue) produce oscillation beams I_1 (blue) and I_3 (green). The depleted I_2 emerging from this interaction is then coupled to the input beam I_5 (red) yielding oscillation beams I_7 (red) and I_6 (green). In this way both oscillation beams produced by the red–green DCPO interaction are affected; i.e. the stronger is the green pump depletion with increasing input blue, the weaker I_6 and I_7 become. On the other hand, the interaction between the input red and green cannot possibly have an effect on the blue–green DCPO process,

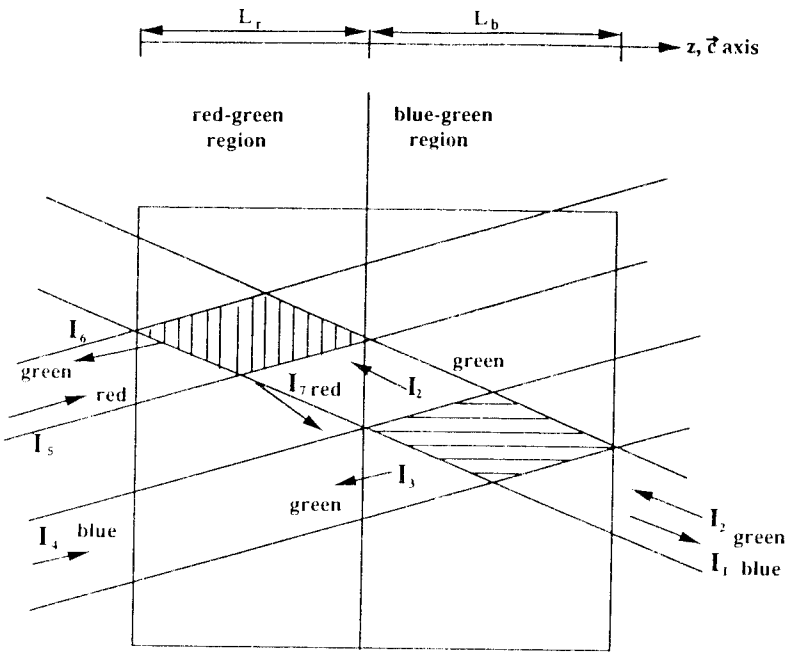

Fig. 2. Schematic diagram of interacting waves in the multi-colour-pumped oscillator.

because according to our model the red beam does not contribute to that process. Such a geometry of interactions was chosen in accordance to the preliminary experimental results described in the previous section.

The development of oscillation beams in such a configuration can be modelled by combining two similar sets of four coupled differential equations; each set describing a single DCPO effect. They can be derived by the slowly-varying-envelope-approximation, discussed in detail in our earlier work [18]. In this first attempt to model the MCPO we shall, for simplicity, restrict ourselves to a one-dimensional theory. The two input beams of two different wavelengths – λ_k and λ_ℓ, are labelled as $A(\lambda_k)$ and $B(\lambda_\ell)$, and the two output oscillation beams are labelled as $C(\lambda_k)$, and $D(\lambda_\ell)$. The resulting differential equations take the form

$$\cos\vartheta_D \frac{dA_D}{dz} = \frac{\gamma_\ell}{I_0}(\xi A_D A_B^* + A_A^* A_C)A_B - \frac{\alpha_\ell}{2}A_D, \tag{1}$$

$$\cos\vartheta_A \frac{dA_A}{dz} = \frac{\gamma_k}{I_0}(\xi A_D^* A_B + A_A A_C^*)A_C + \frac{\alpha_k}{2}A_A, \tag{2}$$

$$\cos\vartheta_C \frac{dA_C}{dz} = -\frac{\gamma_k}{I_0}(\xi A_D A_B^* + A_A^* A_C)A_A + \frac{\alpha_k}{2}A_C, \tag{3}$$

$$\cos\vartheta_B \frac{dA_B}{dz} = -\frac{\gamma_\ell}{I_0}(\xi A_D^* A_B + A_A A_C^*)A_D - \frac{\alpha_\ell}{2}A_B, \tag{4}$$

where

$$I_0 = |A_A|^2 + |A_C|^2 + \xi\{|A_B|^2 + |A_D|^2\}, \tag{5}$$

$$\xi_{\ell k} = s_\ell / s_k, \tag{6}$$

is the ratio of photoexcitation rates for the two incident wavelengths.

α_ℓ and α_k are the absorption coefficients for λ_ℓ and λ_k, respectively. ϑ_i are the angles between output beam i and the c axis. γ_ℓ and γ_k, the coupling coefficients for each wavelength are defined as follows,

$$\gamma_m = \frac{2\pi}{\lambda_m}\frac{r_{\text{eff}}(\lambda_m)n_0^3(\lambda_m)}{2}\frac{E_Q E_T}{E_Q + E_T}, \quad \text{for} \quad m = k, \ell. \tag{7}$$

E_T and E_Q are the diffusion field and the maximum field for a grating of spatial frequency K. r_{eff} is the

FULL LENGTH ARTICLE

effective electro-optic coefficient which can be calculated from the following expression [2],

$$r_{\mathrm{eff}} = \frac{1}{n_{\mathrm{e}} n_{\mathrm{o}}^3} \sin\frac{\vartheta_i + \vartheta_j}{2} \left[n_{\mathrm{o}}^4 r_{13} \cos\vartheta_i \cos\vartheta_j + 2 r_{42} n_{\mathrm{e}}^2 n_{\mathrm{o}}^2 \cos^2\left(\frac{\vartheta_i + \vartheta_j}{2}\right) + n_{\mathrm{e}}^4 \sin\vartheta_i \sin\vartheta_j r_{33} \right], \tag{8}$$

where n_{o} and n_{e} are (ordinary and extraordinary) refractive indices, the electro-optic coefficients r_{13}, r_{42}, and r_{33} are all wavelength dependent. The angles ϑ_i and ϑ_j are between the propagation directions of beams i and j (which form a grating) and the crystal c axis. From the relations given above one can find that:

$$\gamma_{\mathrm{k}} = \frac{\lambda_\ell}{\lambda_{\mathrm{k}}} u_{\mathrm{k}\ell} \gamma_\ell, \tag{9}$$

where

$$u_{\mathrm{k}\ell} = \frac{n_{\mathrm{o}}^3(\lambda_{\mathrm{k}})}{n_{\mathrm{o}}^3(\lambda_\ell)} \frac{r_{\mathrm{eff}}(\lambda_{\mathrm{k}})}{r_{\mathrm{eff}}(\lambda_\ell)}. \tag{10}$$

Our model included two sets of these four coupled differential equations, each adapted appropriately according to the wavelengths and angles used. Thus, in the first set of equations we adjusted the notation for the input blue–green DCPO interaction, i.e. we put $\lambda_{\mathrm{k}} = \lambda_{\mathrm{g}} = 514.5$ nm and $\lambda_\ell = \lambda_{\mathrm{b}} = 488$ nm. Amplitude subscripts A–D were replaced by the labels of waves 1–4 introduced earlier: A by 2, B by 4, C by 3, and D by 1. The second set corresponded to the other, red–green DCPO effect. Hence, the two wavelengths considered here were: the same input green ($\lambda_{\mathrm{k}} = \lambda_{\mathrm{g}} = 514.5$ nm), and the input red ($\lambda_\ell = \lambda_{\mathrm{r}} = 632.8$ nm). Subscripts of amplitudes were also changed appropriately, i.e. A, B, C, D by the labels of waves introduced earlier (Fig. 2): 7, 2, 6, 5. A numerical program was used to solve this two-point boundary-value problem using Newton iteration in a shooting and matching method. We applied the following boundary conditions: $A_1(0) = A_3(L_{\mathrm{b}}) = 0$ with given input values of $A_4(0)$ and $A_2(L_{\mathrm{b}})$ (for the blue–green DCPO), where L_{b} is the length of the region where the blue and green beams interact. For the red–green interaction we shall rescale our coordinate system, which will now range from 0 to L_{r} (L_{r} is the length of the red–green interaction region), and the boundary conditions are $A_7(0) = A_6(L_{\mathrm{r}}) = 0$. The input red beam has an amplitude $A_5(0)$, and the input amplitude of the green beam, $A_2(L_{\mathrm{r}})$ is determined by the first set of differential equations, i.e. it is equal to the output value of the green beam after interaction with the blue input beam. All necessary parameters were evaluated on the basis of the previously determined values. $\gamma_{\mathrm{b}} L_{\mathrm{b}}$ and u_{bg}, and $\gamma_{\mathrm{r}} L_{\mathrm{r}}$ and u_{rg} were used as fitting parameters, varied within the range of the experimental error. The best fit was achieved for their values being approximately within 15% ($\gamma_{\mathrm{b}} L_{\mathrm{b}}$), 4% ($u_{\mathrm{bg}}$), 18% ($\gamma_{\mathrm{r}} L_{\mathrm{r}}$), 3% ($u_{\mathrm{bg}}$) of the values calculated from the material parameters and the angles.

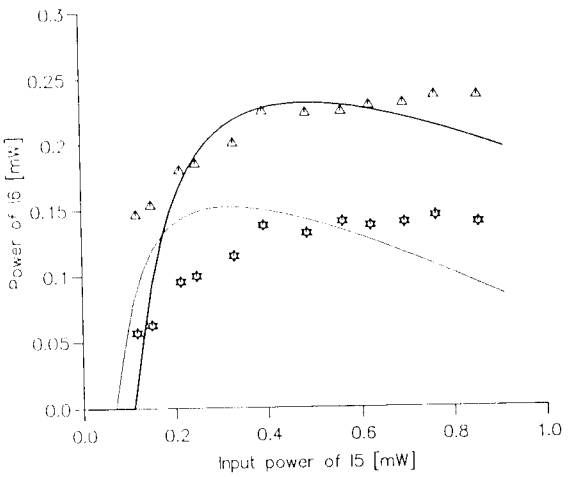

Fig. 3. Observed and calculated power of the green oscillation beam I_6 as a function of input red power I_5. $I_2 = 0.44$ mW. (⋆) and solid curve: input blue, $I_4 = 0.4$ mW is switched on; (△) and solid thick curve: input blue switched off.

The numerical curves presented here have therefore the following parameters: $\gamma_{\mathrm{b}} L_{\mathrm{b}} = 2.5$, $\gamma_{\mathrm{g}} L_{\mathrm{b}} = 2.4$, $\xi_{\mathrm{bg}} = 1.2$, $\alpha_{\mathrm{b}} = 0.44\,\mathrm{cm}^{-1}$, $\alpha_{\mathrm{g}} = 0.34\,\mathrm{cm}^{-1}$; $\gamma_{\mathrm{r}} L_{\mathrm{r}} = 2.0$, $\gamma_{\mathrm{g}} L_{\mathrm{r}} = 2.6$, $\xi_{\mathrm{rg}} = 0.8$, $\alpha_{\mathrm{r}} = 0.25\,\mathrm{cm}^{-1}$, $\alpha_{\mathrm{g}} = 0.34\,\mathrm{cm}^{-1}$.

Figs. 3 and 4 show the mutual influence between the two DCPO effects, observed experimentally and calculated theoretically. As was discussed earlier, the oscillation beams generated in the red–green DCPO interaction, i.e. beams I_6 and I_7 depend on the power of the blue input beam. Fig. 3 presents the power in the green oscillation beam I_6 in the presence and absence of the blue input beam, while the green input power was kept constant. The numerical curves predict quite well the magnitude of change in power, but their shape is slightly different, i.e. they saturate quicker than was

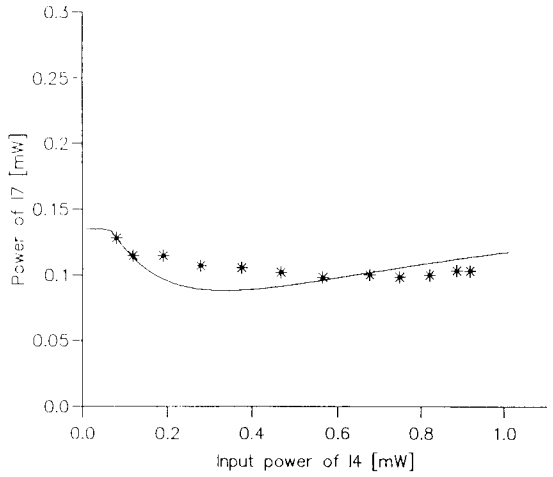

Fig. 4. Red oscillation beam I_7 power versus increasing input blue power. Solid line – theoretical fit to the experimental data (*). $I_5 = 0.55$ mW, $I_2 = 0.38$ mW.

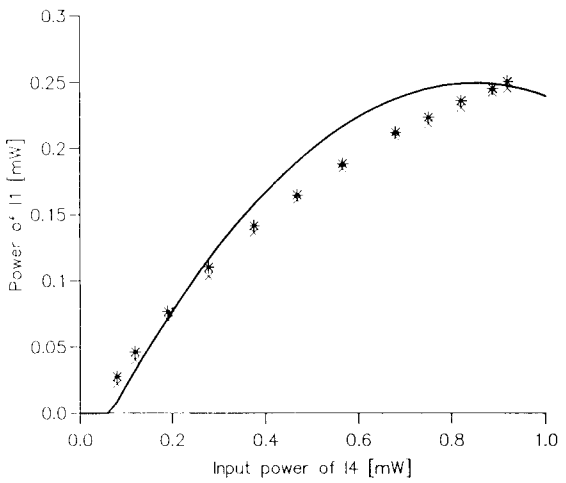

Fig. 5. Power of the blue oscillation beam I_1 variations for increasing input blue. (×): red input I_5 switched off; (*): red input I_5 switched on. Solid line: theoretical fit.

actually measured in the experiment. In Fig. 4 we can see the influence of increasing input blue pump on the red oscillation beam I_7, while both the green and red input powers were kept constant. Both theory and experiment predict a decline in its power. The other oscillation beam coming from the red–green DCPO interaction, I_6, has also been measured and found to vary with blue input in a similar manner.

The power of the blue oscillation beam (I_1) as a function of the blue input beam power (I_4) is shown in Fig. 5, where the solid line represents the theoretical fit. As mentioned before the blue oscillation beam cannot be affected by the red input beam. The experimental results show a very slight dependence on the input red, but it is within the experimental error. Similarly, we can show that increasing input red power does not affect I_1 and I_3. Their value remained constant, within 5%, even for relatively strong input red, i.e. 1 mW. Theoretical values of I_1 and I_3 agree quite well with the experimentally determined values, within about 10%. The comparison presented here and the reasonable agreement between theory and experiment obtained can serve as a basis for different possible arrangements of multi-colour cross coupling. The theoretical model used, assuming only one-dimensional transmission gratings in two separate regions inside the crystal, is very simple indeed. It is worth adding that our theory predicts that if all seven waves share the same interaction region, the oscillation beams will exhibit a totally different behaviour. There would be a very limited range of possible input powers which would allow for four beams to co-exist at the same time, in contrast with our experimental results.

4. Double DCPO phenomenon using an additional probe beam

The experimental arrangement for this type of three-input pumped oscillator is the same as the one presented in Fig. 1, but the red input beam being replaced by another blue beam, to which we refer as the probe beam. A part of the original input blue beam was split and sent towards the crystal as the blue probe beam. Its angle of incidence was approximately equal to that of the input red beam in the previous MCPO.

In this set-up we also observed two DCPO effects giving rise to four oscillation beams – two in green and two in blue. The input blue pump beam (labelled as 4) and the input green (beam 2) generated the oscillation beams in green (beam 3), and in blue (beam 1). The input blue probe (beam 5) and the input green (beam 2) produced another pair of oscillation beams in green (beam 6) and in blue (beam 7). For this configuration of interacting waves we observed, that the power of both oscillation beams originating from the blue–green region, I_1 and I_3, was affected by the inci-

FULL LENGTH ARTICLE

dent blue probe.

We wish to emphasize that the direction of propagation of the beam 7, due to its change in wavelength from red (as was indicated in the diagram) to blue, changed. Beam 7 is less deflected from the green input 2 path than it was in the case of the MCPO. We can actually predict that beam 7 will encounter both the input blue pump 4 and the oscillation beam 1 in the first, blue pump-green DCPO interaction region. These three blue waves are coherent, and evidently their mutual coupling can perturb the DCPO effect. Accordingly we modified the differential equations for waves 4, 1 and 7 by introducing coupling between I_4 and I_7, and between I_1 and I_7 with the aid of the coefficients γ_{47} and γ_{17}. The resulting, new equations for the amplitudes of these three waves will now look as follows,

$$\cos\vartheta_4 \frac{dA_4}{dz} = -\frac{\gamma_b}{I_0}(\xi A_1^* A_4 + A_2 A_3^*)A_1 - \frac{\gamma_{47}}{I_0}\xi A_7 A_7^* A_4 - \frac{\alpha_b}{2}A_4, \tag{11}$$

$$\cos\vartheta_1 \frac{dA_1}{dz} = \frac{\gamma_b}{I_0}(\xi A_1 A_4^* + A_2^* A_3)A_4 - \frac{\gamma_{17}}{I_0}\xi A_7 A_7^* A_1 - \frac{\alpha_b}{2}A_1, \tag{12}$$

$$\cos\vartheta_7 \frac{dA_7}{dz} = \frac{\gamma_{25}}{I_0}(\xi A_7 A_4^* + A_2^* A_3)A_4 + \frac{\gamma_{47}}{I_0}\xi A_4 A_4^* A_7 + \frac{\gamma_{17}}{I_0}\xi A_1 A_1^* A_7 - \frac{\alpha_b}{2}A_7, \tag{13}$$

where I_0 is now

$$I_0 = |A_2|^2 + |A_3|^2 + \xi(|A_4|^2 + |A_1|^2 + |A_7|^2) \tag{14}$$

and γ_{25} is the coupling coefficient between the blue probe and the input green, as defined in Eq. (9).

This modification introduced in the equations of our numerical program enabled us to determine the power of the oscillation beams under the new conditions, and to compare them with the experimental results.

Since the oscillation beams 1 and 7, which were now both in blue, propagated so close to each other, they could not be separated to be measured independently. We will therefore concentrate here on a more detailed analysis of the green oscillation beams. The experimental data may be seen in Fig. 6 and Fig. 7. We increased the input green power and measured the

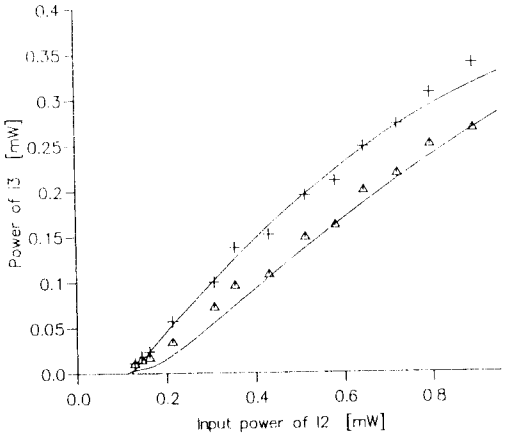

Fig. 6. Experimental and theoretical dependence of the power of the green oscillation beam I_3 on the input green power I_2. (+): input blue probe switched off, (△): input blue probe (I_5 = 0.3 mW) switched on. Solid curves represent theoretical fits. I_4 = 0.5 mW.

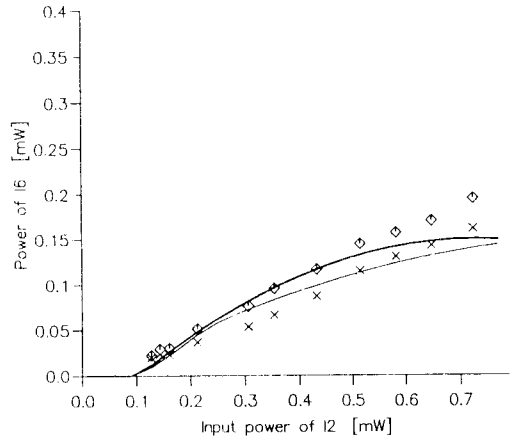

Fig. 7. Power of the green oscillation beam I_6 as a function of increasing input green power I_2 with the input blue pump, I_4 = 0.5 mW present (×) and absent (○). I_5 = 0.3 mW.

power of the two green oscillation beams, I_6 and I_3. For the calculation of the theoretical curves we have used the same parameters as in Sect. 3 for interactions in the first region. Parameters for the new blue probe-green DCPO interaction, and the two coherent two-beam couplings (I_4 with I_7, and I_1 with I_7) were taken as: $\gamma_{25}L_{25} = 2.3$, $\gamma_{47}L_{25} = 2.0$, $\gamma_{17}L_{25} = 0.03$. L_{25} is the interaction length of the input green and the blue probe coupling. γ_{25} was used as a fitting parameter and has been found to be within the same 15%

FULL LENGTH ARTICLE

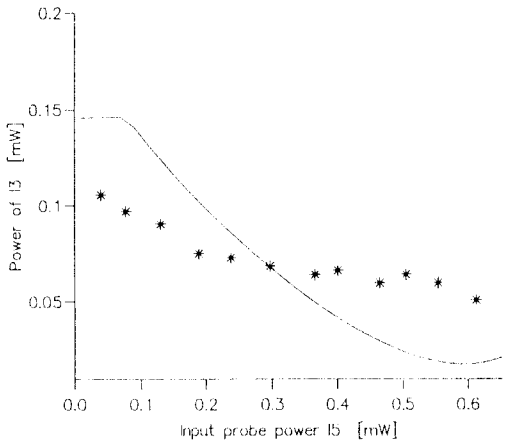

Fig. 8. Dependence of the power of the green oscillation beam I_3 on the input blue probe power I_5 for the double DCPO arrangement. (*): experimental data; solid curve: theoretical prediction.

from the calculated value, similarly like γ_6.

The oscillation beam I_3 (Fig. 6) showed sensitivity to the presence of the input probe – its power declined when the input probe was incident. The corresponding theoretical curves are shown as solid lines. The agreement may be seen to be good. The other oscillation beam in green, I_6, as in the case of the MCPO, decreased in power when the input blue pump was switched on (Fig. 7). The numerical solutions obtained, plotted as solid lines, show the same tendency as the experimental data, but the agreement is less good than for the other oscillation beam (I_3).

In Fig. 8 we plot the power of the oscillation beam in green, I_3, as a function of the input blue probe power. As can be seen, both theory and experiment show a decrease in the I_3 power in the presence of the input blue probe. However, agreement between theory and experiment is only qualitative. We have probably reached the limitations of the one-dimensional theory and for a better agreement, we believe, one should attempt the two-dimensional approach [23,24].

The analysis presented in this section explicitly indicates the destructive influence of the coherent coupling, competing with the DCPO effect. This effect can be in fact expected from previous work [20,22], where the mutual washing-out of multiple-gratings was observed.

5. Conclusions

We have carried out a detailed study of interactions between waves of different wavelengths in a photorefractive material. Two different arrangements have been described. In the first one, multi-colour-pumped oscillator, three different wavelengths were used as three input beams. In the second one, two coherent blue beams were sent on the same side of a photorefractive crystal, and one green beam was incident on its opposite face. We have modelled mathematically both types of interactions with the aid of two interaction regions, each of them represented by a set of four coupled differential equations. In experiments, the power in all four oscillation beams was measured, and then compared with the theoretical predictions. Good agreement between theory and experiment has been found. On the basis of this comparison, it has been shown that the oscillation beams compete for the available input power. The multi-colour-pumped oscillation offers a potentially new application in image colour conversion. Since it is based on the interaction of pump waves of two different colours with the same third wave, the image from this third signal wave can, in principle, be transferred simultaneously into the two different pump wavelengths. Hence, if the signal wave has a wavelength in the visible region, and the two pump waves have different wavelengths, one in the visible and the other in the near-infrared region, it would be possible to arrange an image conversion to both infrared and visible wavelengths at the same time.

Acknowledgments

We wish to thank Ivan Richter for a number of interesting discussions, and Grahame Faulkner for help in setting up the experiment. This work was funded by the Science and Engineering Research Council.

References

[1] B. Fischer and S. Sternklar, Appl. Phys. Lett. 51 (1987) 74.
[2] M. Cronin-Golomb, B. Fischer, J.O. White and A. Yariv, IEEE J. Quantum Electron. 20 (1984) 12

FULL LENGTH ARTICLE

[3] B. Fischer, S. Sternklar and S. Weiss, IEEE J. Quantum Electron. 25 (1989) 550.
[4] M.D. Ewbank, Optics Lett. 13 (1988) 47.
[5] S. Weiss, S. Sternklar and B. Fischer, Optics Lett. 12 (1987) 114.
[6] A.M. Smout, R.W. Eason, Optics Lett. 12 (1987) 498.
[7] S. Sternklar and B. Fischer, Optics Lett. 12 (1987) 711
[8] Qi-Chi He, IEEE J. Quantum Electron. 24 (1988) 2507.
[9] S. Sternklar, S. Weiss, M. Segev and B. Fischer, Optics Lett. 11 (1986) 528; Appl. Optics 25 (1986) 4518.
[10] S. Sternklar, S. Weiss and B. Fischer, Opt. Eng. 26 (1987) 423.
[11] J. Feinberg and G.D. Bacher, Appl. Phys. Lett. 48 (1986) 570.
[12] M. Cronin-Golomb, A. Yariv and I. Ury, Appl. Phys. Lett. 48 (1986) 1240
[13] M. Horowitz, D. Kligler and B. Fischer, J. Opt. Soc. Am. B 8 (1991) 2204.
[14] Q. Byron He and P. Yeh, C. Gu and R.R. Neurgaonkar, J. Opt. Soc. Am. B 9 (1992) 114.
[15] W.R. Christian, R. Saxena and I. McMichael, J. Opt. Soc. Am. B 9 (1992) 108.
[16] D. Statman and B. Liby, J. Opt. Soc. Am. B 6 (1989) 1884.
[17] V. Vieux, P. Gravey, N. Wolffer and G. Picoli, Appl. Phys. Lett. 58 (1991) 2880.
[18] M. Kaczmarek, I. Richter, L. Solymar, J. Opt. Soc. Am. B 11 (1994) 136.
[19] G.W. Ross and R.W. Eason, Optics Lett. 18 (1993) 571.
[20] S.G. Rabbani, J.L. Shults, G.J. Salamo, E.J. Sharp, W.W. Clark III, M.J. Miller, G.L. Wood and R.R. Neurgaonkar, Appl. Phys. B 53 (1991) 323.
[21] H. Kong, M. Cronin-Golomb and B. Fischer, Optics Comm. 93 (1992) 92.
[22] B. Fischer, S. Weiss, S. Sternklar, Appl. Phys. Lett. 50 (1987) 483.
[23] V.V. Eliseev, V.T. Tikhonchuk and A.A. Zozulya, J. Opt. Soc. Am. B 8 (1991) 2497.
[24] N.V. Bogodaev, V.V. Eliseev, L.I. Ivleva, A.S. Korshunov, S.S. Orlov, N.M. Polozkov, A.A. Zozulya, J. Opt. Soc. Am. B 9 (1992) 1493.